ARCTIC
VOL. 72, NO. 3 (SEPTEMBER 2019) P. 245–257
https://doi.org/10.14430/arctic68654

Accelerated Springtime Melt of Snow on Tundra Downwind from Northern Alaska River Systems Resulting from Niveo-aeolian Deposition Events

Gijs de Boer,[1,2,3] Christopher J. Cox,[1,2] and Jessie M. Creamean[1,2,4]

(*Received 14 June 2018; accepted in revised form 27 February 2019*)

ABSTRACT. It is well known that light-absorbing particulate matter (PM) enhances absorption of sunlight when deposited on ice and snow. Such increased absorption is due to a reduction in surface albedo, resulting in accelerated melt of frozen surfaces. In isolation, earlier melt enhances Arctic warming since dark surfaces underlying snow and ice are exposed and absorb additional solar energy. Here, we combine various observational tools to demonstrate that aeolian deposition of PM along fluvial features on the North Slope of Alaska resulted in a notable reduction of surface albedo in the spring of 2016, from values typical for snow (~0.8) to around 0.35 on average. This reduction resulted in accelerated snow and ice melt by up to three weeks compared to unaffected areas. This phenomenon was observed to some degree in 12 other years dating back to 2003. Deposition generally was found to occur near particular sections of the rivers, with several areas affected by events in multiple years. In all years, the deposition is attributed to high wind events. The extreme case in 2016 is linked to unusually strong and extraordinarily persistent winds during April. The deposited material is thought to be the natural sediment carried by the rivers, resulting in a seasonally replenished source of PM. These findings indicate a previously unreported impact of both fluvial and atmospheric processes on the seasonal melt of northern Alaska rivers.

Key words: deposition; albedo; North Slope of Alaska; wind; snow; melt; storm; climate; rivers

RÉSUMÉ. Il s'agit d'un fait bien connu que la matière particulaire photo-absorbante rehausse l'absorption de la lumière solaire lorsqu'elle est déposée sur la glace et la neige. Cette absorption accrue est attribuable à la réduction de l'albédo de la surface, ce qui se traduit par la fonte accélérée des surfaces glacées. Individuellement, la fonte hâtive augmente le réchauffement de l'Arctique parce que les surfaces sombres se trouvant sous la neige et la glace sont exposées et absorbent l'énergie solaire supplémentaire. Ici, nous recourons à divers outils d'observation pour montrer que le dépôt éolien de matière particulaire le long des caractéristiques fluviales de la North Slope de l'Alaska a entraîné une réduction notable de l'albédo de la surface au printemps de 2016, passant de valeurs typiques pour la neige de (~ 0,8) à environ 0,35 en moyenne. Cette réduction a donné lieu à l'accélération de la fonte de la neige et de la glace dans une mesure de trois semaines comparativement aux endroits qui n'ont pas été touchés par la réduction. Ce phénomène a été observé dans une certaine mesure pendant 12 autres années, remontant en 2003. De manière générale, des dépôts se sont ramassés près de segments particuliers des cours d'eau, et plusieurs des secteurs ont été touchés par des événements au cours de plusieurs années. Dans l'ensemble, les dépôts sont attribués à des vents violents. Le cas extrême de 2016 découle de vents inhabituellement forts et extraordinairement persistants en avril. La matière déposée serait peut-être du sédiment naturel transporté par les cours d'eau, ce qui donne lieu au réapprovisionnement saisonnier de la source de matière particulaire. Ces constatations mènent à une incidence antérieurement non déclarée des processus fluviaux et atmosphériques sur la fonte saisonnière des cours d'eau du nord de l'Alaska.

Mots clés : dépôt; albédo; North Slope de l'Alaska; vent; neige; fonte; tempête; climat; cours d'eau

Traduit pour la revue *Arctic* par Nicole Giguère.

[1] Cooperative Institute for Research in Environmental Sciences, University of Colorado Boulder, 216 UCB, Boulder, Colorado 80309, USA
[2] Physical Sciences Division, National Oceanic and Atmospheric Administration, 325 Broadway, Boulder, Colorado 80305, USA
[3] Corresponding author: gijs.deboer@colorado.edu
[4] Current address: Department of Atmospheric Science, Colorado State University, 3915B W. Laporte Ave., Fort Collins, Colorado 80521, USA

INTRODUCTION

Light-absorbing particulate matter (PM) reduces reflectivity (albedo) of frozen surfaces (Clarke and Noone, 1985; Flanner et al., 2007; AMAP, 2011), facilitating acceleration of snow and ice melt by increasing absorption of solar radiation. Such accelerated melt can contribute to climate extremes (Keegan et al., 2014) and variations in hydrology, biogeochemical cycles, and ecological processes (Stone et al., 2002; Prowse et al., 2006; Cox et al., 2017). This melt contributes to a factor in Arctic amplification by enhancing warming through the ice-albedo feedback (IPCC, 2007) whereby dark surfaces underlying snow and ice absorb additional solar energy, further promoting melt.

Previous studies on radiative forcing by absorbing aerosol on Arctic snow and ice have largely focused on deposition onto the surface resulting from long-range transport of PM (Koch and Hansen, 2005; Flanner et al., 2007; McConnell et al., 2007). For example, McConnell et al. (2007) evaluated extended measurements of black carbon from ice cores collected in Greenland to estimate a climate forcing during summer months that increased from approximately 0.42 Wm^{-2} in the pre-industrial era to 1.13 Wm^{-2} during the height of the industrial revolution. The net impact of snow and ice melt resulting from deposition is significantly larger than the direct radiative forcing of the absorbing aerosols themselves, with exposure of bare ground following melt changing net surface radiation at high latitudes by more than 150 Wm^{-2} (Stone et al., 2002). Distant origins of absorbing particles transported to the Arctic have been reported to include biomass burning, and industry and residential emissions (Koch and Hansen, 2005; Stohl et al., 2006; Hegg et al., 2009).

Less attention has been dedicated to the impact of deposition occurring at highly localized scales, where source and deposition regions may be separated by 1 km or less. In addition to impacts from local anthropogenic sources (e.g., Creamean et al., 2018), natural sources include aeolian transport of surface material (Edlund and Woo, 1992) and PM in the region of settlements (Woo and Dubreuil, 1985; Stone et al., 2002) and periglacial environments (Bullard et al., 2016). Work in complex terrain in the vicinity of Ellesmere Island in the Canadian Arctic indicates that deflation of surface sediment by wind followed by on-snow deposition is relatively common, sourced from areas of scoured snow and enhanced by shallow snow cover (Lewkowicz and Young, 1991; Edlund and Woo, 1992). Extreme cases may have lasting effects, as in an example near Eureka, Canada, where a single wind event with gusts reaching up to 40 ms^{-1} was found to be responsible for the equivalent of 20 years' erosion by water in a fluvial system (Lewkowicz, 1998). Additional background on periglacial niveo-aeolian features in parts of Alaska is provided in Ashley et al. (1985) and Bullard et al. (2016), while riverbank activity was previously documented in northern Canada in a pair of studies (Pissart, 1966; Pissart et al., 1977). Additionally, significant work has been completed (e.g., Walker and Everett, 1987; Moorhead et al., 1996; Auerbach et al., 1997; Myers-Smith et al., 2006) to understand the influence of dust transport downwind of transportation infrastructure—such as the gravel roadways supporting resource extraction activities in the Prudhoe Bay oilfields—though much of this work has focused on ecological impacts. While the climate forcing of such intensive short-lived events might be less than that associated with continuous deposition of lower quantities, they can nonetheless have substantial influence on local ecosystems. For example, premature warming of river basins can impact river ice breakup intensity, increased water infiltration into warmed riverbanks, and alter vegetation around river basins (Prowse et al., 2006).

In this study, we provide observational evidence of repeated, localized, intense niveo-aeolian deposition events occurring around river systems on the North Slope of Alaska during spring months, with a focus on the extent of such events and their connection to wind events. One such event, observed in April 2016, provides an extreme example of the potential extent and impact of these occurrences. Moderate Resolution Imaging Spectroradiometer (MODIS) corrected reflectance data from this time show significant deposition of dark material on the North Slope of Alaska (Fig. 1, top). During this time, the most significant deposition occurred from 2–20 April, with accumulation along banks of several North Slope rivers (see details in Fig. 1 and caption). Additionally, Jago River delta deposition resulted in darkening of land fast sea ice and Barter Island, including the village of Kaktovik (Fig. 1D). Finally, deposition was observed along the northern Alaskan coastline, particularly along barrier islands found in this region. Analysis of historical MODIS data reveals additional springtime events with similar features over the past 15 years.

We first provide an overview of datasets and tools used to conduct these analyses, along with a general overview of methodology. This overview is followed by a description of the historical occurrence of river-centric niveo-aeolian deposition events and their connections to regional wind events. Next, we evaluate the 2016 event in further detail, including an assessment of changes to surface albedo and melt timing. Finally, we include discussion on possible impacts of such events and an outlook describing the potential frequency of future events and their impact on the Arctic climate system.

METHODS AND DATASETS

Information from a variety of observational resources is used to complete this analysis. We evaluated the extent of surface deposition by manually reviewing corrected reflectance data from the MODIS instrument operating on the Terra and Aqua satellites, with data obtained from the National Aeronautics and Space Administration (NASA) WorldView webpage (https://worldview.earthdata.nasa.gov).

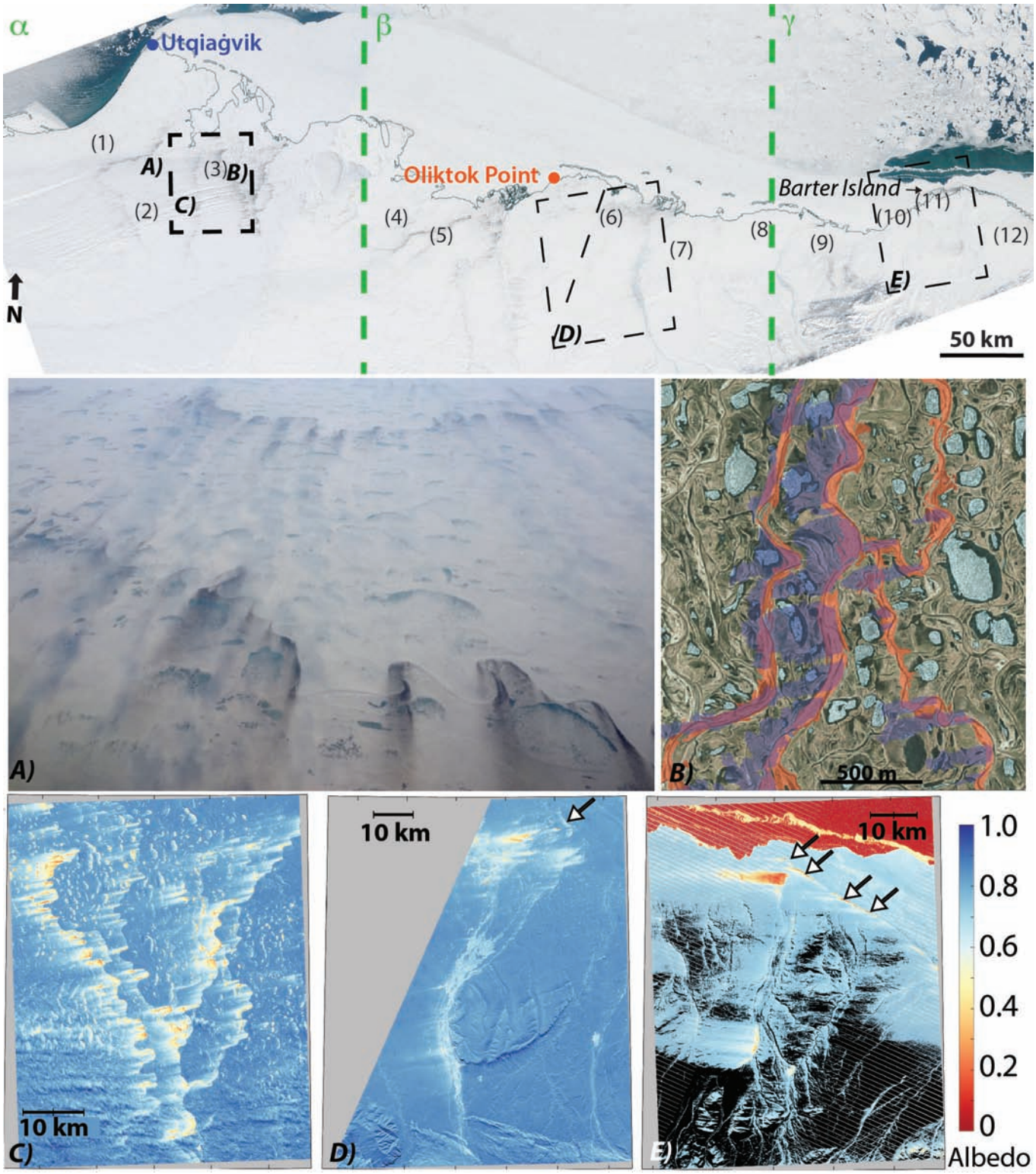

FIG. 1. Top: Northern Alaska, as seen from MODIS on 22 April 2016. Deposited particulate matter (PM) is visible as dark streaks along riverbanks and deltas. Areas showing deposition include (west to east) the banks of the Meade (1), Topagoruk (2), and Chipp and Ikpikpuk Rivers (3), and Fish Creek (4) south and east of Utqiaġvik (formerly Barrow). Additional deposition was observed downwind of the Colville (5) and Sagavanirktok (6) River deltas, and downwind of the Kavik (7), Canning (8), Katakturuk (9), Akutoktak (10), Jago (11), Aichilik and Kongakut Rivers (12) in far northeastern Alaska. Additional PM is visible along coastal barrier islands, particularly east of Barter Island. Numbers in the top image indicate the locations of specific rivers, as named here. Green lines separate the North Slope into three regions (α, β, γ), which correspond with the areas of deposition occurrence in Figure 2. An oblique aerial photograph (panel A on top figure) shows black matter lining riverbanks. Panel B shows a summertime Landsat image, with the riverbeds (orange) and deposition areas (purple) overlaid. Panels C–E show surface albedos derived from Landsat data (12, 13, and 22 April 2016, respectively), for corresponding boxes on the MODIS image. White arrows in panels D and E highlight regions of reduced albedo due to coastal deposition. Areas of missing data in panel E (shaded black) are due to saturation of bands 1 and 3.

Each co-author independently reviewed daily mosaic images covering the entire North Slope of Alaska region. In these reviews, team members identified whether the areas labeled alpha (α), beta (β) and gamma (γ) in Figure 1 were a) cloud covered, and b) showed any signs of surface deposition. Surface deposition was defined and identified as dark features with streak-like appearance oriented in a direction common with the prevailing wind. All dates were reviewed to produce a consensus analysis of these events, and these results were then used to develop the shading in Figure 2.

To evaluate the influence of the observed deposition on surface albedo for an extensive event in 2016, we processed Landsat imagery (30 m) following Wang et al. (2016), who also estimated albedo of snow in Alaska. This imagery was obtained from USGS EarthExplorer (http://earthexplorer.usgs.gov/). Conversion of Landsat near-nadir top-of-atmosphere (TOA) reflectance to surface albedo required several processing steps: (1) an atmospheric correction, (2) a correction for anisotropy, and (3) a narrowband to broadband conversion. Calibration and atmospheric corrections were performed by the Landsat Ecosystem Disturbance Adaptive Processing System (LEDAPS) for Landsat 7 and by the Landsat Surface Reflectance Code (LaSRC) for Landsat 8. Anisotropic scaling is built on Bidirectional Reflectance Distribution Function (BRDF) coefficients from 16-day MODIS (500 m) overpass data provided by the MODIS BRDF (MCD43A) product (Schaaf et al., 2002; Schaaf and Wang, 2015a, b). "RossThick" and "LiSparseReciprocal" kernel weights were used in the BRDF model. Broadband MODIS reflectance at the Landsat viewing and solar geometries was then used to produce nadir-to-albedo reflectance ratios for representative pixels and was applied to the Landsat nadir surface reflectances (Wang et al., 2016). Finally, narrowband surface reflectances were converted to broadband albedo (0.25 – 2.5 μm) using coefficients based on radiative transfer calculations for Landsat 7 (Liang, 2001).

In addition to the Landsat analysis, we used the MODIS white-sky albedo product (i.e., diffuse sky calculation; Schaaf and Wang, 2015a, b) to estimate the day of year when the surface transitioned from snow-covered to snow-free. The albedo threshold used for determination of the date of final snowmelt on the North Slope has historically been set to 0.3 (Foster, 1989; Dutton and Endres, 1991; Stone et al., 2002, 2005; Cox et al., 2017), and detailed justification for this threshold can be found in the referenced articles. When melt occurs, the albedo rapidly falls from about 0.75 (at initiation of melt) to about 0.3 (final melt) and the climatological average duration of this time period at Utqiaġvik is 5 ± 2.4 days (Cox et al., 2017). In 2016, the melt was relatively fast: At Utqiaġvik the 0.3 threshold was reached in two days and at Oliktok Point, the albedo fell to 0.4 in two days, although it lingered just above 0.3 for about another six days. Conversely, the albedo for determination of the onset of snowpack during autumn has previously been set to 0.6 (Cox et al., 2017). Part of the reason for the choice of 0.6 is that measured albedo is somewhat noisy and so it is desirable to set the threshold outside of the range of the noise. Given the coarseness of the spatial and temporal resolution of the MODIS images analyzed in the current work, it is believed that the initiation of melt is more readily identified using the upper end of the albedo range encountered during melt (which is more homogeneous) than using the date of the final melt (which is very localized). Specifically, some pixels in the vicinity of Utqiaġvik and Oliktok Point show a prolonged period with albedo between about 0.3 and 0.6. While this delay could be interpreted as analogous to what was observed at the Oliktok station in 2016, it seems to be unrealistically prolonged. The leveling off of the MODIS data above 0.3 could be caused by a variety of factors, including real spatial variability in melting of the snowpack within the MODIS pixel. However, more spurious factors could also be to blame, including patches of snow drifts, the influence of lake ice on the high density of small lakes on the North Slope, which typically melts sometime in July (Cox et al., 2017), and smoothing of the time series caused by the influence of 16-day composites that are used for the MODIS product. For these reasons, we use a threshold of 0.6 to represent a date closer to the initiation of melt.

To support evaluation of satellite data and provide meteorological context for periods connected to deposition events, we used surface meteorological and radiation data from two U.S. Department of Energy Atmospheric Radiation Measurement (DOE ARM) program sites at Utqiaġvik (North Slope of Alaska; NSA) and Oliktok Point (Third ARM Mobile Facility; AMF-3), Alaska (ARM, 2016a, b). These data were obtained from the DOE ARM data archive (http://www.archive.arm.gov/armlogin/login.jsp). Additionally, we evaluated meteorological observations and surface albedo (calculated from irradiance data) from the National Oceanic and Atmospheric Administration (NOAA) Global Monitoring Division (GMD), Utqiaġvik observatory (http://www.esrl.noaa.gov/gmd/dv/data/index.php?site=brw). ARM albedo data were calculated using solar-noon irradiance values, based on data from the Quality Controlled Radiation (QCRAD) product (ARM, 2016a). Comparison of surface- and satellite-based albedo estimates resulted in agreement to within 1% using nearby pixels in the Landsat 8 image shown in Figure 1B. Comparison of the MODIS-derived melt dates at the nearest pixels to Utqiaġvik and Oliktok Point to those derived from the station albedo measurements showed agreement to within three days. Further, surface (10 m) wind measurements from the DOE ARM sites were evaluated to quantify the magnitude of wind events and their timing relative to the appearance of deposited material. Evaluation of these data included historical detection of strong wind events, considering both speed and direction impacts. Additionally, we provide further context on the degree that the 2016 wind event and subsequent extensive surface deposition were anomalous relative to other years by calculating persistence of daily mean winds based on consecutive occurrences at a specific wind speed

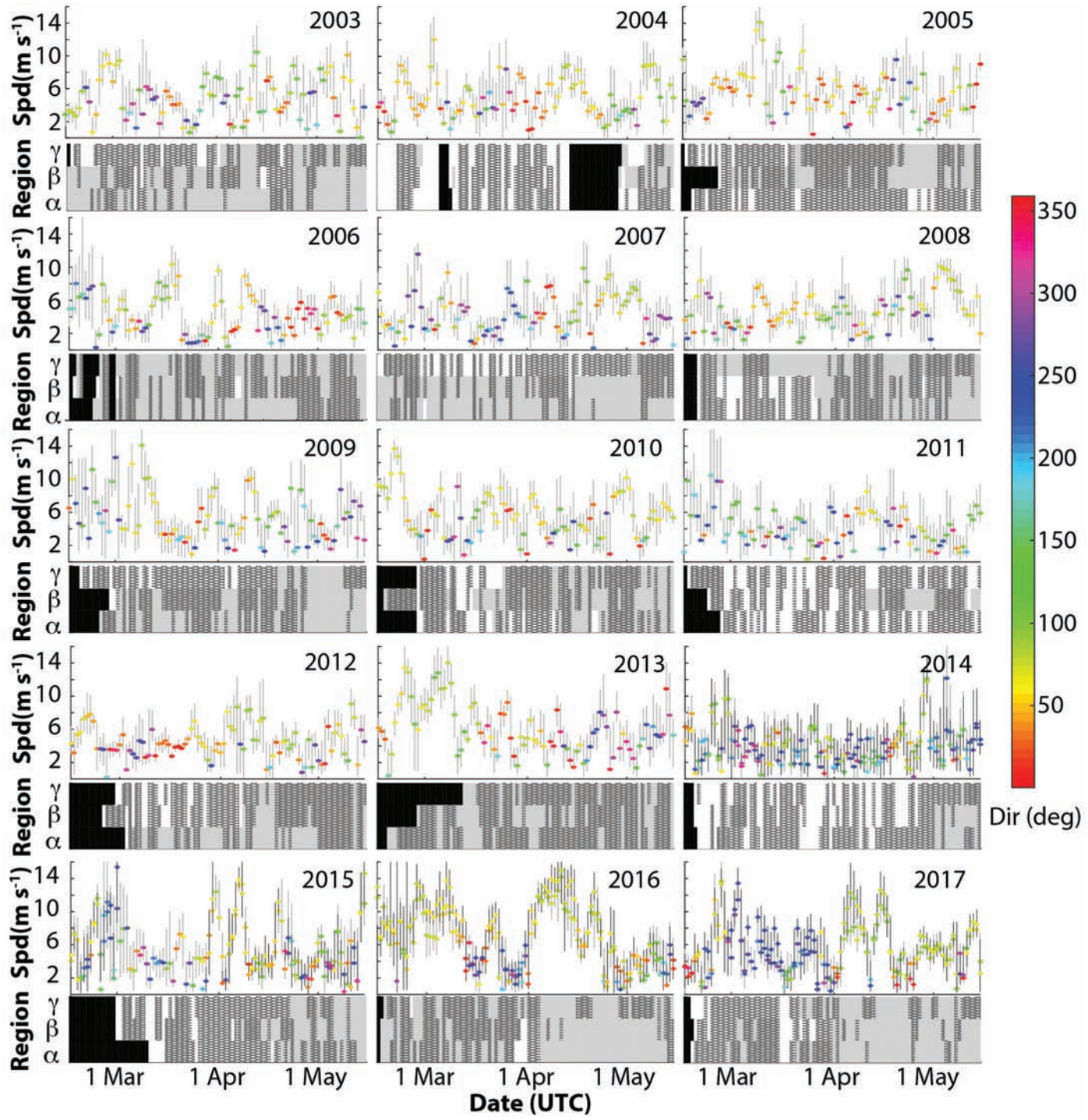

FIG. 2. A historical perspective on wind speeds from surface meteorological measurements at Utqiaġvik (2003–17) and Oliktok Point (2014–17) is included in the top panel for each year. Ovals, colored by wind direction, show daily mean wind speeds; bars show maximum and minimum hourly mean winds for a given day. The bottom panels provide information on deposition presence, as detected through analysis of daily MODIS imagery, for the river features present in the three regions (α, β, γ) indicated in Figure 1. Grey areas represent time periods with deposition, while white areas indicate time periods when no deposition was observed. Black areas indicate either missing data or years where the first days of the analysis period are cloud covered, or both. Black hatching indicates periods of cloud cover when the surface was not observable. During these cloud-covered periods, the last-known surface condition is assumed to persist until the surface is again visible.

and by assessing the historical frequency of occurrence of similar wind events through a long-term evaluation at the Utqiaġvik facility, where ARM has been measuring surface winds for over 20 years.

RESULTS

Evaluation of historical (2003–17) springtime (15 February–15 May) niveo-aeolian deposition and its connection to wind intensity and duration (Fig. 2) illustrates the conditions under which these events occurred.

First, most years had some level of niveo-aeolian deposition, and this deposition was almost exclusively present around river features, with additional niveo-aeolian deposition occurring along coastal barrier islands. Certain years had more persistent presence of the deposited materials than others. In general, the appearance of darkened snow around rivers occurred during time periods with elevated east-northeasterly wind intensities. For years that include wind measurements from both Oliktok Point and Utqiaġvik (2014 – 17), daily wind speeds from the two sites were correlated with one another (R^2 of 0.49). Similarly, historical evaluation of daily wind speed measurements from National Weather Service sites at the Utqiaġvik, Deadhorse, and Nuiqsut airports also revealed high correlations (R^2 of 0.58, 0.65, and 0.88), with Deadhorse and Nuiqsut having the highest correlation. These results are not surprising because the wind patterns on the North Slope are dominated by northeasterly winds driven by large-scale circulation around the Beaufort High (Stegall and Zhang, 2012).

A second item to note is that some regions for which deposition is identified early in the season were later classified as not having deposition. Such occurrences took place after cloudy periods during which fresh snow had likely fallen and covered previously visible material. However, once deposition was noted, dark material on the snow was generally observed for much of the remainder of the season or, if covered by snowfall, often reappeared with subsequent wind events. Most years transitioned to some level of deposition occurring towards the end of the year.

Finally, it is notable that deposition did not occur uniformly across the North Slope. Along with the zonal variability identified, each region featured specific "hot spots" where deposition occurred on a semi-regular basis. These hot spots include (from west to east) the Topagoruk, Chipp, and Ikpikpuk Rivers, the Sagavanirktok River west of Franklin Bluffs, and the deltas of the Okpilak and Jago Rivers (Fig. 1). It is important to note that the Franklin Bluffs hotspot may see enhancement in dust deposition due to the co-location of the Dalton Highway with the Sagavanirktok River in this area, though focused analysis of this region shows deposition occurring both up- and downwind of the highway. Also, it is interesting to note that all of these hotspots are downstream of a substantial area of aeolian silt, as identified in a recent ecological mapping of the North Slope of Alaska (Jorgenson and Grunblatt, 2013). While the deposition observed in 2016 was more extreme than other years, its spatial distribution (Fig. 1, top) was broadly representative of the hot spots that appeared in other years.

Having detected niveo-aeolian deposition and the meteorological conditions driving it, we next focus on 2016 as an example of an extreme event (see Fig. 1). A review of MODIS imagery and surface-based meteorological data revealed that peak deposition occurred in the first half of April 2016, coinciding with anomalously windy conditions in northern Alaska. During this period, the National Centers for Environmental Prediction and the National Center for Atmospheric Research (NCEP/NCAR) reanalysis indicated a large area of high pressure over the Beaufort Sea, resulting in strong regional northeasterly winds. Surface (10 m) winds at Oliktok Point (ARM, 2016b) from 0Z 3 April to 0Z 16 April 2016 showed winds averaged 12.6 ms^{-1}, with a maximum 1-minute average of 20.5 ms^{-1}. Similarly, NSA winds (ARM, 2016b) averaged 11.1 ms^{-1} with a maximum 1-minute average of 18.7 ms^{-1}. Evaluation of 1000 mb winds from the North American Regional Reanalysis (NARR; Mesinger et al., 2006) showed elevated wind speeds extending inland across the region. While the absolute wind speeds were not unprecedented, comparison with historical NOAA GMD data (1994-present; NOAA, 2018) revealed that the persistence of elevated wind speeds was very anomalous, with the two-week mean wind velocity being greater than the 95th percentile of all two-week periods, and daily average wind at 8, 9, or 10 ms^{-1} persisting for 13, 11, and 9 days, respectively, all of which have only been exceeded one other time over the past 22 years. The combination of strong winds and extended persistence of these winds was enough to scour substantial amounts of snow from the surface, both exposing the underlying riverbed materials and resulting in their saltation and suspension. This wind-driven mechanism for deposition was evidenced by the northwest-to-southeast (i.e., downwind) dispersion pattern of the deposited material that appeared in the MODIS and Landsat imagery coincident with the wind event. The orientation of this dispersion pattern was similar to that seen in other years, and the location of the deposition demonstrates fluvial origins of the deposited PM (Fig. 1B; Fig. 3A, B).

The presence of the material on the snow-covered tundra significantly darkened the surface, as demonstrated by an aerial photograph (Fig. 1A). Analysis of Landsat data showed that the observed deposition notably impacted surface albedo, with a drop from values typical of snow-covered surfaces (0.75 – 0.85) in unaffected areas to much lower values (0.3 – 0.4) in deposition areas (Fig. 1C – E; Fig. 3A). Evaluation of broadband (0.4 – 4 μm) solar irradiance measurements from the DOE ARM Utqiaġvik and Oliktok Point observatories (ARM, 2016a), as well as those from the NOAA GMD observatory, did not show similar albedo decreases. NSA and AMF-3 albedos during this time ranged from 0.74 – 0.89 and 0.77 – 0.87, respectively, consistent with satellite estimates over areas without notable deposition. This demonstrates the highly localized nature of the deposition and supports a strong connection to non-vegetated surfaces along the tundra-covered North Slope of Alaska, generally limited to riverbeds and barrier island beaches.

Satellite measurements showed accelerated spring albedo/reflectance reductions associated with the accelerated melt of snow cover where deposition occurred compared to the surrounding region (Figs. 3 and 4). In areas where substantial reductions in albedo were observed by satellite,

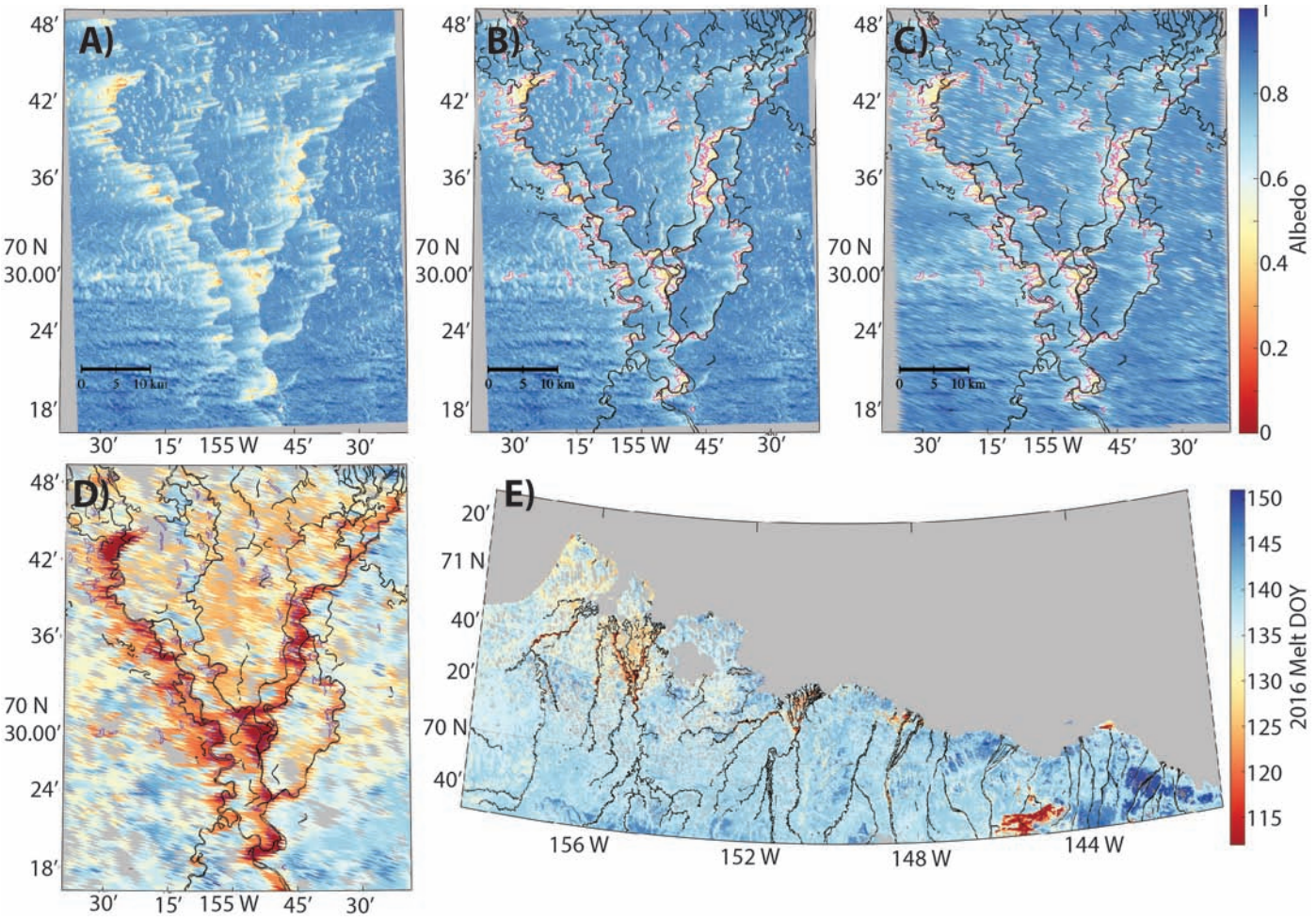

FIG. 3. Panel A shows surface albedo, as calculated from a single Landsat image on 12 April 2016 at the native Landsat resolution. Panel B is the same image, with the addition of contours highlighting the location of riverbeds (black lines) and areas identified as having significant deposition by an albedo threshold of 0.6 (pink lines) on this date. Panel C is the same as panel B, except the resolution has been degraded to match that of MODIS. Panels A–C share the upper colorbar to the right of panel C. Panel D shows the same region with the same black contours as panels B and C, though the pink contours have been made purple for clarity against the background. The colored shading in panel D represents the day of year (DOY) when melt occurred, based on the same 0.6 threshold, but now from the MODIS white sky albedo product. Light grey pixels indicate lake features that are masked out; dark grey pixels are those that had not exceeded the 0.6 threshold by 30 May, possibly also because ice covered the lakes. Finally, panel E is the same MODIS melt DOY estimate for the entire North Slope. River locations are areal hydrographic features that include streams, rivers, and areas of complex channels from the USGS National Hydrography Dataset (NHD), available from the USDA at https://gdg.sc.egov.usda.gov/GDGOrder.aspx.

evaluation of clear sky periods (Fig. 4) and the white sky albedo product from MODIS (Fig. 3), from April and May 2016, indicated a notable acceleration of albedo reduction relative to surrounding areas. Impacted areas revealed localized bare tundra as early as 2 May 2016 (DOY 122), with more general exposure of the darker tundra surface by 10 May 2016 (DOY 130) in the visible imagery in Figure 4. These areas passed the 0.6 albedo threshold used to indicate a transition from a snow-covered surface to one without snow well ahead of the deposition-free regions, which did not experience extensive albedo reductions until 20 May 2016 (DOY 140) or later. That the areas with earlier albedo reductions align nearly perfectly with areas that featured reduced albedos after the deposition events before any melt had occurred in early April (Fig. 3) indicates a link between the initial deposition-based darkening of the surface and the eventual accelerated transition to a snow-free surface. The temporal progression illuminated through this analysis implies acceleration of melt by up to three weeks in impacted areas compared to the surrounding region.

DISCUSSION

Niveo-aeolian events such as those detected in the current study are influential on local ecosystems along the North Slope of Alaska, as previously discussed in relation to road dust events (e.g., Moorhead et al., 1996; Auerbach et al., 1997; Myers-Smith et al., 2006) and the impact of fluvial floodplain dust on soil alkalinity (Walker et al., 1998). In addition to these ecological impacts, the change in surface albedo associated with these events appears to result in a larger melt date anomaly than the one week suggested by artificial dust-on-snow experiments in a high Arctic location (Edlund and Woo, 1992).

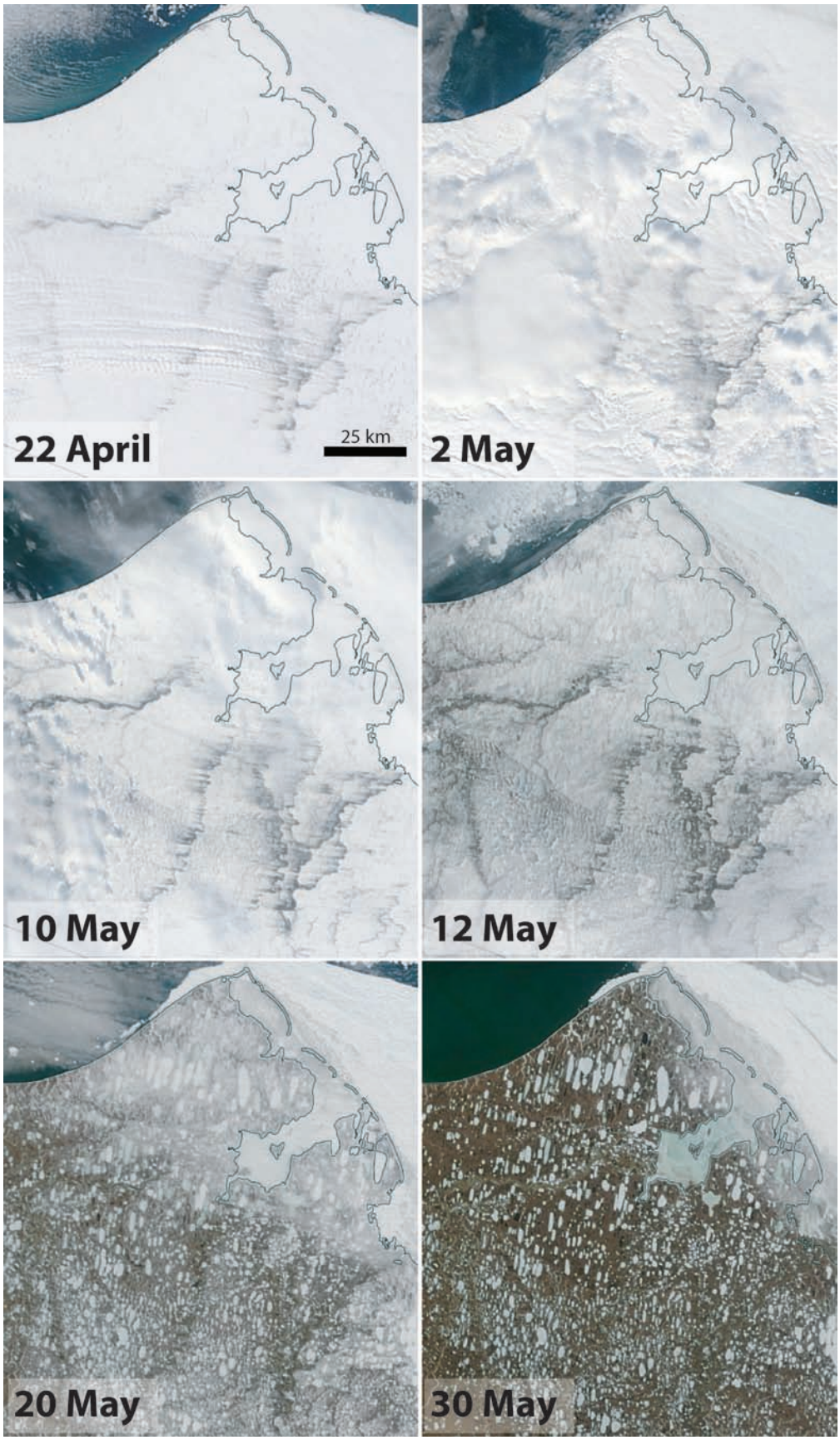

FIG. 4. Sequential MODIS corrected reflectance images illustrating inferred melt in the area south of Utqiaġvik in spring 2016. Note the accelerated disappearance of snow in the river regions where substantial surface deposition was observed, starting with the 10 May image and extending through the end of the melt season. Semi-transparent white features seen on all dates are the result of thin cloud cover.

While connections to wind speed and direction are demonstrated, the exact wind speed required to trigger an event is dependent upon a number of additional factors, including river bed composition and grain size, snow cover, surface moisture content, and snow age. Geological analysis of North Slope rivers indicates that sands of these rivers are composed of various mineral compounds. Based on a survey of the Sagavanirktok River, Robinson and Johnsson (1997) found a primary composition including calcite, quartz, and sedimentary and metasedimentary lithic fragments, with the relative amounts of these compounds evolving with distance from the Brooks Range. The headwaters of the Sagavanirktok were noted to include Devonian through Permian black shales, quartzose sandstones, chert-rich conglomerates, and platform carbonates. The grain size distribution was bimodal, with one mode in the pebble to cobble range, and the second mode falling in the medium sand range (0.25 – 0.5 mm diameter). The first, larger mode has been noted in other studies (e.g., Lamb and Toniolo, 2016) and is unlikely to contribute significantly to observed deposition events because of the large mass of these particles and the force required to suspend and redistribute them on top of snow.

The median grain size reported by Lamb and Toniolo (2016) was in the coarse to very coarse gravel range (27 – 65 mm diameter), a range that has only been observed to be transported by wind elsewhere in the Arctic by rare extreme high-wind events (Lewkowicz, 1998). However, the medium sand mode identified by both studies could be transported by saltation or in suspension by winds (at 10 m height above the surface) of less than 10 ms^{-1} based on a simple relationship between friction velocity and the fluid threshold shear velocity (Bagnold, 1941). These values are estimated without sufficient consideration of complicating, but unknown factors, including particle shape, soil compaction, surface moisture, and snow pack characteristics (McKenna Neuman, 1993). The snow pack can both reduce deposition if deep snow covers the riverbed, as well as enhance it through kinetic transfer between blowing snow and the riverbed surface (e.g., Dietrich, 1977a, b; McKenna Neuman, 1989). Colder air temperatures in this part of the world can impact the extent of transport at a given wind speed, with increased air density supporting transport at lower wind speeds (Selby et al., 1974; Pye and Tsoar, 1990). This appears to be contradictory to our finding of enhanced deposition towards the end of the season (April), when temperatures should be increasing (and air density decreasing).

Seasonal resupply of fluvial sands by river-flow modulation provides opportunities for annual deposition events. The general lack of vegetation in riverbeds and turbulence induced by their topography both work to enhance localized transport and nearby downwind deposition. The meandering, braided nature of North Slope rivers and their deltas provides numerous opportunities for collection and redistribution of sedimentary materials. Additionally, along-coast deposition is supported by barrier island formation processes in this region (Hopkins and Hartz, 1978; Short, 1979). Since fresh river outflow has a lower density than the salt water it is flowing into, it stays near the top of the water column and is directly influenced by wind-driven surface currents. Evaluation of the NCEP/NCAR atmospheric reanalysis and Utqiaġvik and Oliktok Point wind data shows that July – October 2015 winds were predominantly northeasterly along the Beaufort Sea coastline, resulting in transport of fluvial outflow to the barrier islands during the summer and fall.

While previous studies indicate that most PM deposition events in Alaska occur in autumn (Bullard et al., 2016), the present analysis identifies localized springtime deposition having direct consequences on the spring snowmelt period around river systems. In general, timing of spring deposition events plays an important role in the magnitude of melt. Early-season events are less prone to enhanced melt because of substantially colder temperatures, lower sun angles, and shorter daylight hours. Additionally, the overlying atmosphere itself contains an increased number of scattering particulates resulting from the seasonal "Arctic haze" present in February and March. This haze reduces the influence of surface albedo on absorption of solar radiation, since the airborne particles scatter and reflect radiation before it reaches the surface. Similarly, clouds impact the net absorbed shortwave at the surface by shading, an effect termed shortwave cloud radiative forcing. This forcing is small when the albedo of the surface is similar to that of the cloud (such as when snow is present), limiting its effect on absorbed shortwave. Consequently, even when ample sunlight returns, clouds on the North Slope continue to have little influence in the shortwave until after the surface albedo is decreased by seasonal melting of snow (Dong et al., 2010; Cox et al., 2017). The presence of on-snow deposition shown here signals a localized role for clouds in shortwave surface radiative forcing earlier in the season, whereby their net cooling effect over areas with deposition constitutes a negative feedback on the localized melt.

The melt associated with these deposition events could have a significant impact on Arctic river hydrology, geomorphology, and ecology by accelerating the melting of river ice (Pavelsky and Zarnetske, 2017) and the surrounding snow surfaces, ultimately resulting in an earlier river breakup and higher likelihood of early season flooding. Given the potential for an increase in extreme ice-season wind events (Manson and Solomon, 2007) with a changing climate, the likelihood of these events could increase in a warming climate. In isolation, surface darkening by this phenomenon would act as a positive feedback on Arctic warming, resulting in potential positive feedback loops between these events and the elements driving them. Additionally, there could be positive feedbacks involving reductions in vegetation resulting from the downwind deposition on leaves, increasing the likelihood of future deflation in the un-vegetated area (Edlund and Woo, 1992).

Substantial questions still exist on the modulators and sources of these cold-region aeolian events (e.g., McKenna Neuman, 1993; Bullard et al., 2016). Notably, most previous work has focused on periglacial environments. In Alaska, niveo-aeolian deposits have been analyzed in proglacial dunes on the Seward Peninsula (Koster and Dijkmans, 1988) and periglacial environments in the southeast, but to our knowledge have not previously been reported for non-glacial environments (see Bullard et al., 2016) as we demonstrate here. Bullard et al. (2016) attributed PM plumes in southeast Alaska to mesoscale wind events that primarily deflate material of small size, resulting in both local and distant transport. Conversely, relatively coarser material in the non-glacial northern Alaskan riverine systems falls into the upper end of the size distribution of high-latitude aeolian "dust" transport reported by Bullard et al. (2016) and thus is transported only locally by wind on the North Slope. However, the wind events associated with this transport are synoptic in scale rather than mesoscale, and consequently we find that a widespread region experiences the associated effects simultaneously.

It is notable that some of the events described here are superimposed upon anomalously early melting of snow cover along the broader North Slope in recent years. Historical albedo records from Utqiaġvik, which date back to the early 20th century (Cox et al., 2017), show that 2016 was the earliest recorded melt in the North Slope area and 2015 was the 4th earliest melt date. Thus, the three-week anomaly reported here for the riverine systems, which is relative to the surrounding region during the time of melt, is actually likely to be significantly larger climatologically. Since 80% of the years analyzed in this study exhibited deposition, those years showing a lack of deposition (e.g., 2011) may also be climatologically impactful with unusually late snowmelt anomalies (plausibly associated with above-average snow depth or below-average winds) within the "hot spot" regions prone to the deposition. While full evaluation of all vulnerabilities and the potential for multi-year impacts from a single deposition event will require additional study across a variety of disciplines, this work demonstrates that the impact of Arctic wind events can extend far beyond their occurrence and, in combination with dark fluvial material, can impact the spring melt of North Slope river systems.

SUMMARY

Evidence presented demonstrates the regional impact of high wind events on the albedo of snow surrounding northern Alaskan river systems through niveo-aeolian deposition events and the subsequent melt of darkened snow surfaces. These events are responsible for a reduction in springtime surface albedo of up to 45% downwind of river features, resulting in accelerated melt of snow and ice in areas of deposition by up to three weeks, compared to surrounding areas and alteration of the timing of river thaw and breakup. Such events appeared to be influential in at least some regions in 12 of the 15 years for which MODIS data is available. A general link to high wind events is demonstrated, with an apparent directional dependence, with deposition events largely linked to strong east-northeasterly flow, such as that associated with strong Beaufort High events offshore. Ultimately, the extent to which individual areas are impacted appears to be a combined function of the atmospheric pattern governing the occurrence of high wind events and fall ocean currents, river structure and location relative to major topographical features, and the annual cycles of fluvial sediment transport and precipitation.

The current observational network provides only qualitative insight into the occurrence and extent of these deposition events. Future targeted studies, including dense surface meteorological networks and surface albedo surveys, potentially in the hotspots identified in this paper, could provide significant insight into the extent of events, wind-speed thresholds associated with deposition events, and the subsequent melt progression during late spring. Additionally, enhanced river flow networks could help demonstrate links between deposition amount, river thaw, and seasonal flow rate in impacted areas. Such studies would greatly help to answer questions raised by the current qualitative documentation of these features across the North Slope of Alaska.

ACKNOWLEDGEMENTS

We would like to acknowledge significant discussions on topics related to this paper with William Neff, Ryan Spackman, Amy Solomon, Allison McComiskey, Maximilian Maahn, Robert Stone, John Daniel, and the late Andrew Slater. Additionally, we would like to acknowledge funding from the following sources: The U.S. Department of Energy Atmospheric Systems Research Program (grants: DE-SC0013306 and DE-SC0011459), the National Science Foundation Office of Polar Programs (grant: ARC 1203902) and the Arctic Research Program of the NOAA Climate Program Office. The datasets used in this analysis were supported and available through the hard work of the U.S. Department of Energy's Atmospheric Radiation Measurement (ARM) program, the NOAA Global Monitoring Division (GMD) and the National Aeronautics and Space Administration WorldView project.

REFERENCES

Ashley, G.M., Shaw, J., and Smith, N.D., eds. 1985. Glacial sedimentary environments, SEPM Short Course No. 16. Tulsa, Oklahoma: Society of Economic Paleontologists and Mineralogists.

AMAP (Arctic Monitoring and Assessment Programme). 2011. The impact of black carbon on Arctic climate. By Quinn, P.K., Stohl, A., Arneth, A., Bemtsen, T., Burkhart, J.F., Christensen, J., Flanner, M., Kupiainen, K., Lihavainen, H., Shepherd, M., Shevchenko, V., Skov, H., and Vestreng, V. AMAP Technical Report 4. Oslo: AMAP. 72 p.

ARM (Atmospheric Radiation Measurement Climate Research Facility). 2016a. Quality-controlled radiation product (QCRAD1LONG). 2016-04-02 to 2016-04-20, 71.32 N, 156.52 W and 70.495 N, 149.886 W: North Slope Alaska (NSA) and ARM Mobile Facility (OLI) Oliktok Point, Alaska; AMF3 processed data. Compiled by C. Long. ARM data archive, updated hourly. Oak Ridge, Tennessee: ARM. https://www.archive.arm.gov/discovery

———. 2016b. Surface meteorological instrumentation (MET). 2016-04-01 to 2016-04-30, 70.495 N 149.886 W: ARM Mobile Facility (OLI) Oliktok Point, Alaska; AMF3 (M1) and 71.323 N 156.609 W: North Slope Alaska (NSA) Central Facility, Barrow, AK (C1). Compiled by D. Holdridge and J. Kyrouac. ARM data archive. Oak Ridge, Tennessee: ARM.

Auerbach, N.A., Walker, M.D., and Walker, D.A. 1997. Effects of roadside disturbance on substrate and vegetation properties in Arctic tundra. Ecological Applications 7(1):218–235. https://doi.org/10.1890/1051-0761(1997)007[0218:EORDOS]2.0.CO;2

Bagnold, R.A. 1941. The physics of blown sand and desert dunes. London: Methuen.

Bullard, J.E., Baddock, M., Bradwell, T., Crusius, J., Darlington, E., Gaiero, D., Gassó, S., et al. 2016. High-latitude dust in the Earth system. Reviews of Geophysics 54(2):447–485. https://doi.org/10.1002/2016RG000518

Clarke, A.D., and Noone, K.J. 1985. Soot in the Arctic snowpack: A cause for perturbations in radiative transfer. Atmospheric Environment 19(12):2045–2053. https://doi.org/10.1016/0004-6981(85)90113-1

Cox, C.J., Stone, R.S., Douglas, D.C., Stanitski, D.M., Divoky, G.J., Dutton, G.S., Sweeney, C., George, J.C., and Longenecker, D. 2017. Drivers and environmental responses to the changing annual snow cycle of northern Alaska. Bulletin of the American Meteorological Society 98(12):2559–2577. https://doi.org/10.1175/BAMS-D-16-0201.1

Creamean, J.M., Maahn, M., de Boer, G., McComiskey, A., Sedlacek, A.J., and Feng, Y. 2018. The influence of local oil exploration and regional wildfires on summer 2015 aerosol over the North Slope of Alaska. Atmospheric Chemistry and Physics 18(2):555–570. https://doi.org/10.5194/acp-18-555-2018

Dietrich, R.V. 1977a. Wind erosion by snow. Journal of Glaciology 18(78):148–149. https://doi.org/10.3189/S0022143000021614

———. 1977b. Impact abrasion of harder by softer materials. Journal of Geology 85(2):242–246. https://doi.org/10.1086/628289

Dong, X., Xi, B., Crosby, K., Long, C.N., Stone, R.S., and Shupe, M.D. 2010. A 10 year climatology of Arctic cloud fraction and radiative forcing at Barrow, Alaska. Journal of Geophysical Research 115, D17212. https://doi.org/10.1029/2009JD013489

Dutton, E.G., and Endres, D.J. 1991. Date of snowmelt at Barrow, Alaska, U.S.A. Arctic and Alpine Research 23(1):115–119. https://doi.org/10.1080/00040851.1991.12002827

Edlund, S.A., and Woo, M.-K. 1992. Eolian deposition on western Fosheim Peninsula, Ellesmere Island, Northwest Territories during the winter of 1990–91. Current Research, Part B, Interior Plains and Arctic Canada. Geological Survey of Canada Paper 92-1B. 91–96. https://doi.org/10.4095/132840

Flanner, M.G., Zender, C.S., Randerson, J.T., and Rasch, P.J. 2007. Present-day climate forcing and response from black carbon in snow. Journal of Geophysical Research 112, D11202. https://doi.org/10.1029/2006JD008003

Foster, J.L. 1989. The significance of the date of snow disappearance on the Arctic tundra as a possible indicator of climatic change. Arctic and Alpine Research 21(1):60–70.

Hegg, D.A., Warren, S.G., Grenfell, T.C., Doherty, S.J., Larson, T.V., and Clarke, A.D. 2009. Source attribution of black carbon in Arctic snow. Environmental Science & Technology 43(11):4016–4021. https://10.1021/es803623f

Hopkins, D.M., and Hartz, R.W. 1978. Coastal morphology, coastal erosion, and barrier islands of the Beaufort Sea, Alaska. Open File Report 78-1063. Washington, D.C.: U.S. Department of the Interior, Geological Survey.

IPCC (Intergovernmental Panel on Climate Change). 2007. AR4 climate change 2007: Synthesis report. In: Core Writing Team, Pachauri, R.K., and Reisinger, A., eds. Contribution of Working Groups I, II and III to the Fourth Assessment Report of the Intergovernmental Panel on Climate Change. Geneva, Switzerland: IPCC. 104 p.

Jorgenson, M.T., and Grunblatt, J. 2013. Landscape-level ecological mapping of northern Alaska and field site photography. Fairbanks, Alaska: Arctic Landscape Conservation Cooperative, U.S. Fish and Wildlife Service. http://alaskaaga.gina.alaska.edu/catalog/entries/3870-landscape-level-ecological-mapping-of-northern

Keegan, K.M., Albert, M.R., McConnell, J.R., and Baker, I. 2014. Climate change and forest fires synergistically drive widespread melt events of the Greenland Ice Sheet. Proceedings of the National Academy of Sciences 111(22):7964–7967. https://doi.org/10.1073/pnas.1405397111

Koch, D., and Hansen, J. 2005. Distant origins of Arctic black carbon: A Goddard Institute for Space Studies ModelE experiment. Journal of Geophysical Research 110, D04204. https://doi.org/10.1029/2004JD005296

Koster, E.A., and Dijkmans, J.W.A. 1988. Niveo-aeolian deposits and denivation forms, with special reference to the great Kobuk Sand Dunes, northwestern Alaska. Earth Surface Processes and Landforms 13(2):153–170. https://10.1002/esp.3290130206

Lewkowicz, A.G. 1998. Aeolian sediment transport during winter, Black Top Creek, Fosheim Peninsula, Ellesmere Island, Canadian Arctic. Permafrost and Periglacial Processes 9(1):35–46. https://doi.org/10.1002/(SICI)1099-1530(199801/03)9:1<35::AID-PPP276>3.0.CO;2-L

Lewkowicz, A.G., and Young, K.L. 1991. Observations of aeolian transport and niveo-aeolian deposition at three lowland sites, Canadian Arctic Archipelago. Permafrost and Periglacial Processes 2(3):197–210. https://doi.org/10.1002/ppp.3430020304

Lamb, E., and Toniolo, H. 2016. Initial quantification of suspended sediment loads for three Alaska North Slope rivers. Water 8(10):419. https://10.3390/w8100419

Liang, S. 2001. Narrowband to broadband conversions of land surface albedo I: Algorithms. Remote Sensing of Environment 76(2):213–238. https://doi.org/10.1016/S0034-4257(00)00205-4

Manson, G.K., and Solomon, S.M. 2007. Past and future forcing of Beaufort Sea coastal change. Atmosphere-Ocean 45(2):107–122. https://doi.org/10.3137/ao.450204

McKenna Neuman, C.M. 1989. Kinetic energy transfer through impact and its role in entrainment by wind of particles from frozen surfaces. Sedimentology 36(6):1007–1015. https://doi.org/10.1111/j.1365-3091.1989.tb01538.x

———. 1993. A review of aeolian transport processes in cold environments. Progress in Physical Geography: Earth and Environment 17(2):137–155. https://doi.org/10.1177/030913339301700203

McConnell, J.R., Edwards, R., Kok, G.L., Flanner, M.G., Zender, C.S., Saltzman, E.S., Banta, J.R., Pasteris, D.R., Carter, M.M., and Kahl, J.D.W. 2007. 20th-century industrial black carbon emissions altered Arctic climate forcing. Science 317(5843):1381–1384. https://10.1126/science.1144856

Mesinger, F., DiMego, G., Kalnay, E., Mitchell, K., Shafran, P.C., Ebisuzaki, W., Jović, D., et al. 2006. North American regional reanalysis. Bulletin of the American Meteorological Society 87(3):343–360. https://doi.org/10.1175/BAMS-87-3-343

Moorhead, D.L., Linkins, A.E., and Everett, K.R. 1996. Road dust alters extracellular enzyme activities in tussock tundra soils, Alaska, U.S.A. Arctic and Alpine Research 28(3):346–351. https://doi.org/10.1080/00040851.1996.12003187

Myers-Smith, I.H., Arnesen, B.K., Thompson, R.M., and Chapin, F.S. 2006. Cumulative impacts on Alaskan Arctic tundra of a quarter century of road dust. Ecoscience 13(4):503–510. https://doi.org/10.2980/1195-6860(2006)13[503:CIOAAT]2.0.CO;2

NOAA (National Oceanic and Atmospheric Administration). 2018. Surface meteorological data. 1994-01-01 to 2018-01-01, 71.32 N, 156.61 W: Barrow Observatory (BRW) processed data. NOAA Earth System Research Laboratory, Global Monitoring Division data archive. https://www.esrl.noaa.gov/gmd/dv/ftpdata.html

Pavelsky, T.M., and Zarnetske, J.P. 2017. Rapid decline in river icings detected in Arctic Alaska: Implications for a changing hydrologic cycle and river ecosystems. Geophysical Research Letters 44(7):3228–3235. https://doi.org/10.1002/2016GL072397

Pissart, A. 1966. Le rôle géomorphologique du vent dans la région de Mould Bay (Ile Prince Patrick – N.W.T. – Canada). Zeitschrift für Geomorphologie 10:226–236.

Pissart, A., Vincent, J.-S., and Edlund, S.A. 1977. Dépôts et phénomènes éoliens sur l'île de Banks, Territoires du Nord-Ouest, Canada. Canadian Journal of Earth Sciences 14(11):2462–2480. https://doi.org/10.1139/e77-214

Prowse, T.D., Wrona, F.J., Reist, J.D., Gibson, J.J., Hobbie, J.E., Levesque, L.M.J., and Vincent, W.F. 2006. Climate change effects on hydroecology of Arctic freshwater ecosystems. AMBIO: A Journal of the Human Environment 35(7):347–358. https://doi.org/10.1579/0044-7447(2006)35[347:CCEOHO]2.0.CO;2

Pye, K., and Tsoar, H. 1990. Aeolian sand and sand dunes. London: Unwin Hyman.

Robinson, R.S., and Johnsson, M.J. 1997. Chemical and physical weathering of fluvial sands in an Arctic environment: Sands of the Sagavanirktok River, North Slope, Alaska. Journal of Sedimentary Research 67(3):560–570. https://doi.org/10.1306/D42685D1-2B26-11D7-8648000102C1865D

Schaaf, C., and Wang, Z. 2015a. MCD43A1 MODIS/Terra+Aqua BRDF/Albedo model parameters daily L3 Global 500m V006 [Data set]. NASA EOSDIS Land Processes DAAC. https://doi.org/10.5067/MODIS/MCD43A1.006

———. 2015b. MCD43A3 MODIS/Terra+Aqua BRDF/Albedo daily L3 Global – 500m V006 [Data set]. NASA EOSDIS Land Processes DAAC. https://doi.org/10.5067/MODIS/MCD43A3.006

Schaaf, C.B., Gao, F., Strahler, A.H., Lucht, W., Li, X., Tsang, T., Strugnell, N.C., et al. 2002. First operational BRDF, albedo nadir reflectance products from MODIS. Remote Sensing of Environment 83(1-2):135–148. https://doi.org/10.1016/S0034-4257(02)00091-3

Selby, M.J., Rains, R.B., and Palmer, R.W.P. 1974. Eolian deposits of the ice-free Victoria Valley, southern Victoria Land, Antarctica. New Zealand Journal of Geology and Geophysics 17(3):543–562. https://doi.org/10.1080/00288306.1973.10421580

Short, A.D. 1979. Barrior island development along the Alaskan–Yukon coastal plains. Geological Society of America Bulletin 90:77–103. https://doi.org/10.1130/gsab-p2-90-77

Stegall, S.T., and Zhang, J. 2012. Wind field climatology, changes, and extremes in the Chukchi–Beaufort Seas and Alaska North Slope during 1979–2009. Journal of Climate 25(23):8075–8089. https://doi.org/10.1175/JCLI-D-11-00532.1

Stohl, A., Andrews, E., Burkhart, J.F., Forster, C., Herber, A., Hoch, S.W., Kowal, D., et al. 2006. Pan-Arctic enhancements of light absorbing aerosol concentrations due to North American boreal forest fires during summer 2004. Journal of Geophysical Research 111, D22214. https://doi.org/10.1029/2006JD007216

Stone, R.S., Dutton, E.G., Harris, J.M., and Longenecker, D. 2002. Earlier spring snowmelt in northern Alaska as an indicator of climate change. Journal of Geophysical Research 107, D10, 4089. https://doi.org/10.1029/2000JD000286

Stone, R.S., Douglas, D.C., Belchansky, G.I., and Drobot, S.D. 2005. Correlated declines in Pacific Arctic snow and sea ice cover. Arctic Research of the United States 19:18–25.

Walker, D.A., and Everett, K.R. 1987. Road dust and its environmental impact on Alaskan taiga and tundra. Arctic and Alpine Research 19(4):479–489. https://doi.org/10.1080/00040851.1987.12002630

Walker, D.A., Auerbach, N.A., Bockheim, J.G., Chapin, F.S., III, Eugster, W., King, J.Y., McFadden, J.P., et al. 1998. Energy and trace-gas fluxes across a soil pH boundary in the Arctic. Nature 394:496–472. https://doi.org/10.1038/28839

Wang, Z., Erb, A.M., Schaaf, C.B., Sun, Q., Liu, Y., Yang, Y., Shuai, Y., Casey, K.A., and Román, M.O. 2016. Early spring post-fire snow albedo dynamics in high latitude boreal forests using Landsat-8 OLI data. Remote Sensing of Environment 185:71–83. https://doi.org/10.1016/j.rse.2016.02.059

Woo, M.-K., and Dubreuil, M.-A. 1985. Empirical relationship between dust content and Arctic snow albedo. Cold Regions Science and Technology 10(2):125–132. https://doi.org/10.1016/0165-232X(85)90024-2